3-5 March 1987
pp. 205 - 212

Sensor and Simulation Notes
Note 289
28 August 1985

The Distributed Switch for Launching Spherical Waves

Carl E. Baum
Air Force Weapons Laboratory

D.V. Giri
Pro-Tech, 125 University Ave., Berkeley, CA 94710

Abstract

One way of launching a fast transient pulse in the TEM mode of a biconic (or monoconic) antenna geometry is to use a distributed source. This paper discusses and generalizes this concept to that of a distributed switch which can be incorporated in typical Marx/peaker geometries. Various shapes for this type of distributed source/switch are also discussed.

Contents

I. Introduction

Over the years research into techniques for launching transient electromagnetic (EM) waves has yielded various results incorporated into the design of EMP simulators [9]. As one goes to higher-voltage sources (pulse power) then the electric fields near a single-output-switch source become larger. The breakdown-electric-field strength of the air and of other media (gases, oil, etc.) limits the magnitude of the allowable electric fields.

The size of the source (near the output switch(es)) also can limit the rise time of the desired EM wave in or around the simulator. When a switch (in general involving an arc to close the switch) closes, it takes time for this closure to be effective in establishing a new electric field around the switch because of the finite velocity of transient EM propagation. In this context the size of the switch itself can become important as its size increases to switch larger and larger voltages.

As voltages become larger one can reduce the voltage on an individual closing switch by increasing the number of switches. However, these switches can close at various relative times, influencing the character of the resulting EM wave (at least at early times) launched on the simulator. The problem is to construct an array of switches which close at appropriate times to produce the desired EM wave.

What this leads to is the concept of a distributed source which "matches" the desired EM wave. Distributed sources can come in various forms depending on the type of desired EM wave. In this note our concentration is on such distributed sources for launching spherical waves on rotationally symmetric conducting conical systems [1,2]. These can also be extended to the inhomogeneous TEM waves on cylindrical or conical systems [3,4,5,6], or plane waves [7,8]. In these studies, it is clear that the separation (or size) of the individual elements (including switches as a part) limits

the early-time or high-frequency performance of the distributed source. Of course the basic switch performance is also a factor, but this is a different issue.

This note discusses some nuances of distributed sources for launching rotationally-symmetric spherical waves. In particular it discusses the combination of this distributed-source concept with traditional circular biconic (or monoconic) pulse-generator/ wave-launching systems.

II. Concept of Distributed Source

The basic concept of the distributed source is related to the EM uniqueness theorem. As is well known in EM theory [11], the solution for the EM fields in a volume is determined by the fields on the associated boundary surface. The surface fields of concern are the tangential (to the surface) electric and magnetic fields. While various combinations are possible, it is the tangential electric field which is our immediate concern. It is sufficient that the tangential electric field on the boundary surface be chosen (and produced) which is associated with the desired electromagnetic fields (of course, satisfying the Maxwell equations) in the volume of interest.

The basic theory for such a source is given in [1]. For present purposes let us summarize the basic fields here. Referring to fig. 2.1 we have cartesian (x,y,z), cylindrical (Ψ,ϕ,z), and spherical (r,θ,ϕ) coordinate systems, related by

$$\begin{aligned} x &= \Psi\cos(\phi) = r\sin(\theta)\cos(\phi) \\ y &= \Psi\sin(\phi) = r\sin(\theta)\sin(\phi) \\ z &= r\cos(\theta) \\ \Psi &= r\sin(\theta) \end{aligned} \tag{2.1}$$

The expanding spherical wave of interest is TEM of the form (for $\theta_o < \theta < \pi - \theta_o$)

$$\begin{aligned} \vec{E} &= E_\theta \vec{1}_\theta = \frac{V_o}{r} f_E(\theta)\, f(t - \frac{r}{c}) \\ \vec{H} &= H_\phi \vec{1}_\phi = \frac{1}{Z_o}\frac{V_o}{r} f_E(\theta)\, f(t - \frac{r}{c}) \end{aligned} \tag{2.2}$$

$$Z_o = \sqrt{\frac{\mu_o}{\varepsilon_o}} \quad \text{(wave impedance of free space)}$$

$$c = \frac{1}{\sqrt{\mu_o \varepsilon_o}} \quad \text{(speed of light)}$$

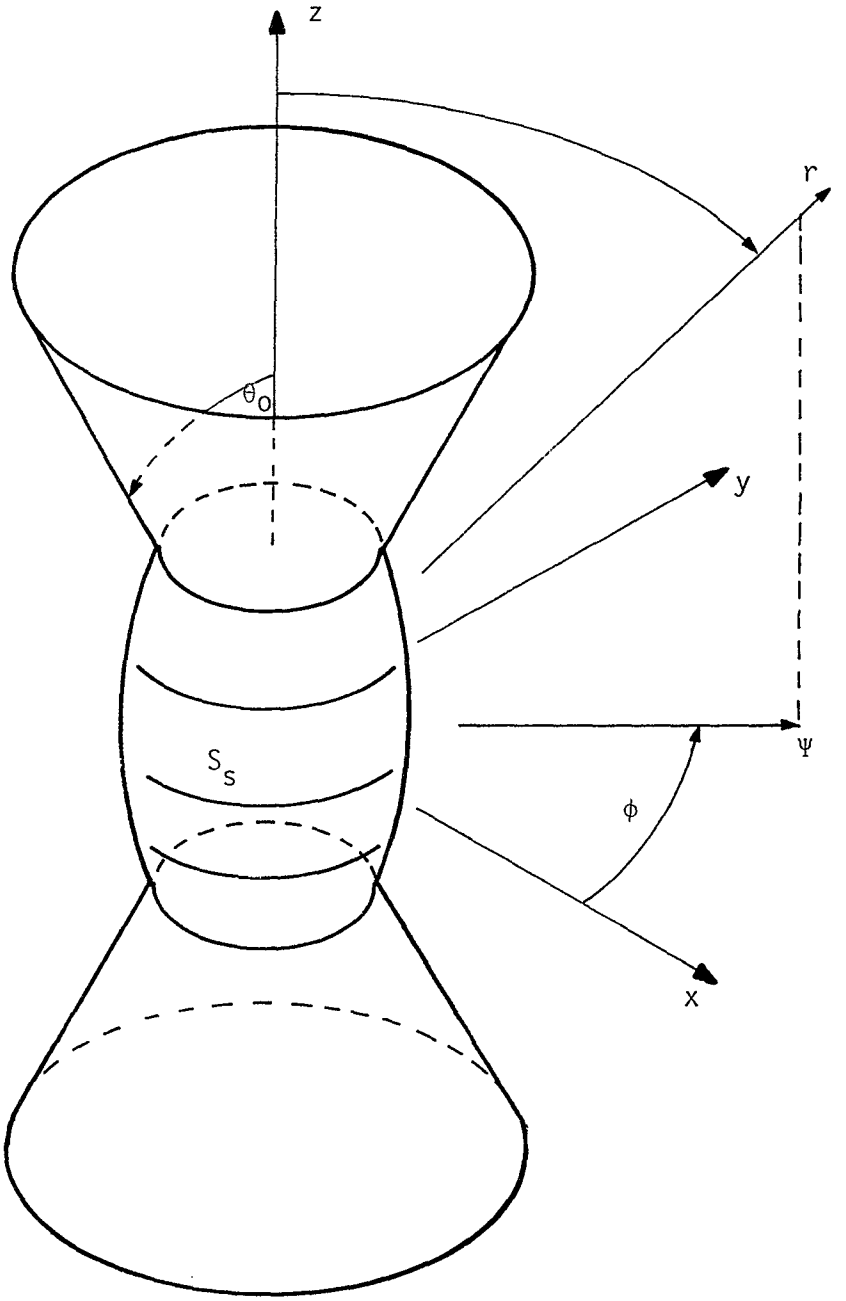

Figure 2.1. Source Surface with Symmetrical Bicone

The θ dependence is

$$f_E(\theta) = \left\{\sin(\theta)\, \ell n\left[\cot\left(\frac{\theta_o}{2}\right)\right]\right\}^{-1}$$

$$\int_{\theta_o}^{\pi-\theta_o} f_E(\theta)d\theta = 2 \qquad (2.3)$$

This is related to a potential function (voltage)

$$V = V_o f_V(\theta)\, f(t - \frac{r}{c})$$

$$\frac{df_V(\theta)}{d\theta} = -f_E(\theta) \qquad (2.4)$$

$$f_V(\theta) = \frac{\ell n\left[\tan\left(\frac{\theta}{2}\right)\right]}{\ell n\left[\tan\left(\frac{\theta_o}{2}\right)\right]} = \frac{\ell n\left[\cot\left(\frac{\theta}{2}\right)\right]}{\ell n\left[\cot\left(\frac{\theta_o}{2}\right)\right]}$$

$$f_V(\theta_o) = 1,\ f_V(\tfrac{\pi}{2}) = 0\ ,\quad f_V(\pi - \theta_o) = -1$$

Here the formulae are in terms of free-space parameters, but by using more general (constant) ε and μ , the results apply to other media as well. Note that V_o is a convenient scaling voltage; $2V_o$ is the voltage between the two cones, or V_o is the voltage of one cone ($\theta=\theta_o$) with respect to a ground plane ($\theta = \pi/2$) if a monocone system is being considered. Typically we can choose $f(t - \frac{r}{c})$ in a normalized form with a peak value of about one.

As discussed in [1] it is only required that the component of the desired $\vec{E}$ (as in (2.2)) be enforced on a source surface S_s for EM fields in the volume of interest ($\theta_o < \theta < \pi - \theta_o$ and $\vec{r}$ "outside" S_s) to be those originally desired (as the EM fields described above). This is the fundamental concept of a distributed

source for launching a spherical TEM wave for this case of rotation symmetry, or by extension for other kinds of spherical TEM waves (other forms of $f_E(\theta,\phi)$). In essence the idea is to extrapolate the desired EM fields (of course assumed to satisfy the Maxwell equations in the media of interest) back to appropriate boundaries on which sources are provided to at least approximate the tangential component of the desired electric field in both space and time (or frequency) on S_s.

III. Typical Circular-Biconic (or Monoconic) Marx/Peaker Geometries.

Over the years there has been some evolution of the technology of the design of pulse generators to drive EMP simulators. As discussed in [10] one of the common configurations of pulsers to drive a circular biconic system is that illustrated in fig. 3.1. Here the peaking capacitors form part of the circular conical structure as a wave-guiding structure (approximate conductor) for the high frequencies. Note that there are many peaker arms (not shown) to approximate a body of revolution.

The discussion here is not concerned with the theory of peaking capacitors, but with distributed sources. Note that in the typical pulser system in fig. 3.1 a gas enclosure is used to increase the dielectric strength of the region near the switch with high electric fields. The peak electric fields at the surface of the gas enclosure are of the order of one MV/m (allowing for the dielectric strength of air with some derating). As one approaches the switch region in the high-dielectric-strength gas additional enclosures with higher pressure high-dielectric-strength gas can also be used to accomodate the higher electric fields. Eventually one encounters the switch(es) proper from which the fast-rising EM wave is to be launched.

Arriving at the switch region, the physical size of the switch can limit the rise characteristics of the EM wave due to transit-time effects across the switch. One can try to reduce the size of the switch to reduce such problems. Alternately (and complementarily) one can attempt to design the switch to minimize such problems. One approach to this is to segment the switch into a larger number of smaller switches which synthesize the desired EM wave over the switch region. Such is the subject of this paper.

Note that while fig. 3.1 shows the case of a symmetrical circular bicone, by inserting a ground plane through the center of the switch region and normal to the $\mathcal{C}$ of the pulser one has a circular monoconic geometry to which the current discussion equally applies. In the case of a monoconic geometry one has the choice of placing the Marx and

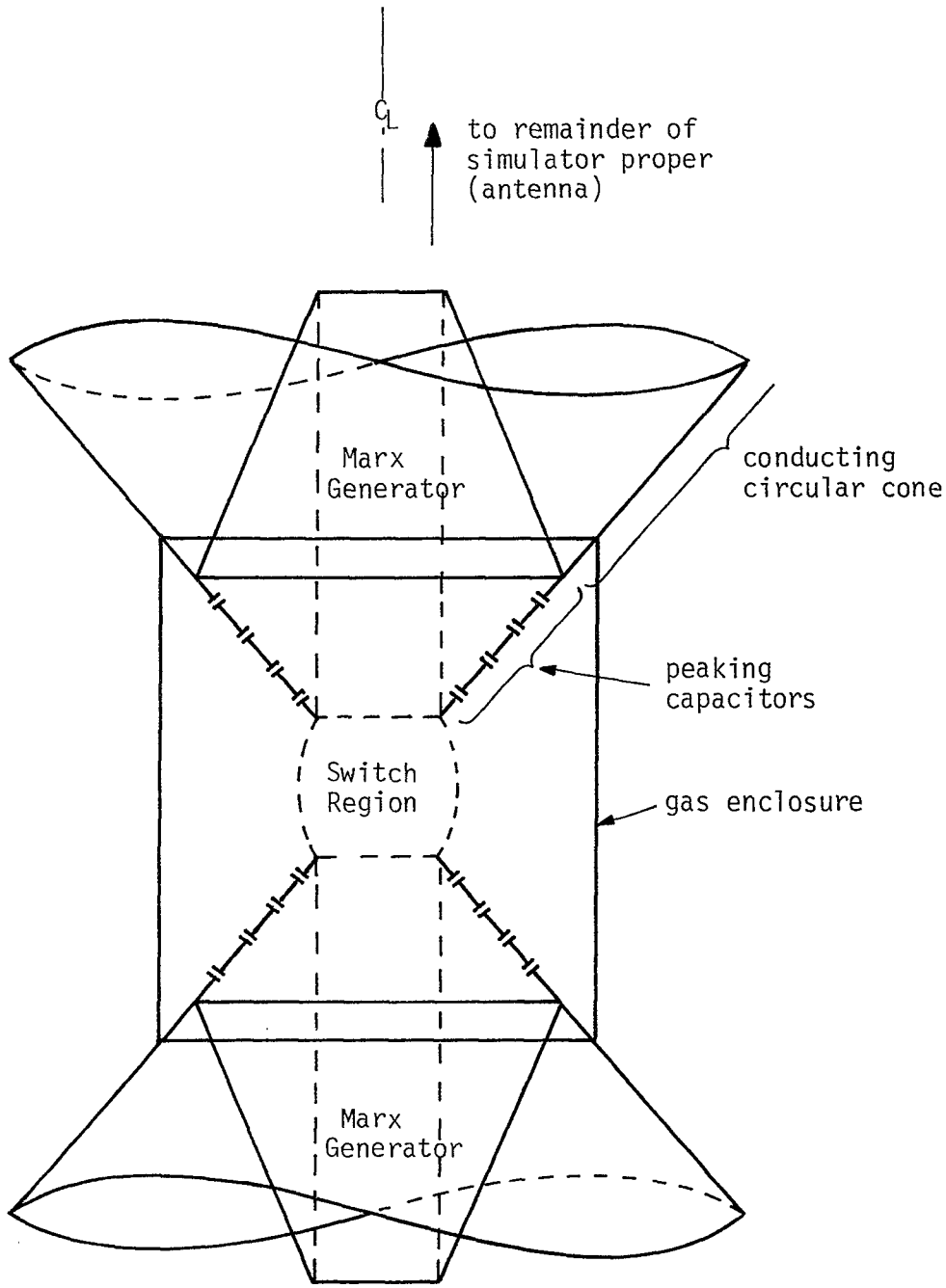

Figure 3.1. Divided Marx Generator in Circular-Biconic Geometry with Peaking-Capacitor Arms as Part of Bicone Waveguide

peaking capacitors in the cone as shown, or alternately in and below the ground plane which has been introduced. However, these options do not affect the essentials of the discussion here.

IV. The Distributed-Source Concept as a Distributed Switch

Beginning with the distributed source concept in section 2 let us suppose that there is some set of sources (say charged capacitors) with switches on a source surface S_s (say a circular cylinder) as illustrated in fig. 4.1A. Here the cylinder has radius Ψ_1, length h_1, and typical tangential-electric-field magnitude E_1 (say near $\theta = \pi/2$ or the symmetry plane orthogonal to the cylinder axis). Now S_s might be chosen so that outside S_s might be air and E_1 might be of the order of one MV/m. Of course one could also move the distributed source farther back toward the coordinate center ($\vec{r} = \vec{0}$) and this is in effect what the distribued switch does.

Note that the distributed source with a set of sources distributed near S_s also launches an inward propagating wave with a line focus on the z axis. This field on the z axis can be transiently larger in magnitude than E_1 and prudent design precautions may be needed to minimize this potential problem.

Let the sources on S_s be spaced a distance Δ_1 in the z direction and δ_1 in the ϕ direction, with these spacings being sufficiently small to maintain a sufficiently small rise time (or sufficiently large high-frequency performance) of the desired spherical TEM wave in section 2. Then the number of sources (including switches) for this distributed source is given by

$$N_1 = \frac{h_1}{\Delta_1} \frac{2\pi\Psi_1}{\delta_1} \tag{4.1}$$

Contrast the previous distributed source with the distributed switch illustrated in fig. 4.1B. In this case the distributed switch is in general of much smaller size. Let the switches on the new S_s of length h_2 and radius Ψ_2 be spaced a distance Δ_2 in the z direction and δ_2 in the ϕ direction, again with these spacings small enough to maintain the requisite early-time (or high-frequency) performance. Then the number of switches for this distributed switch is given by

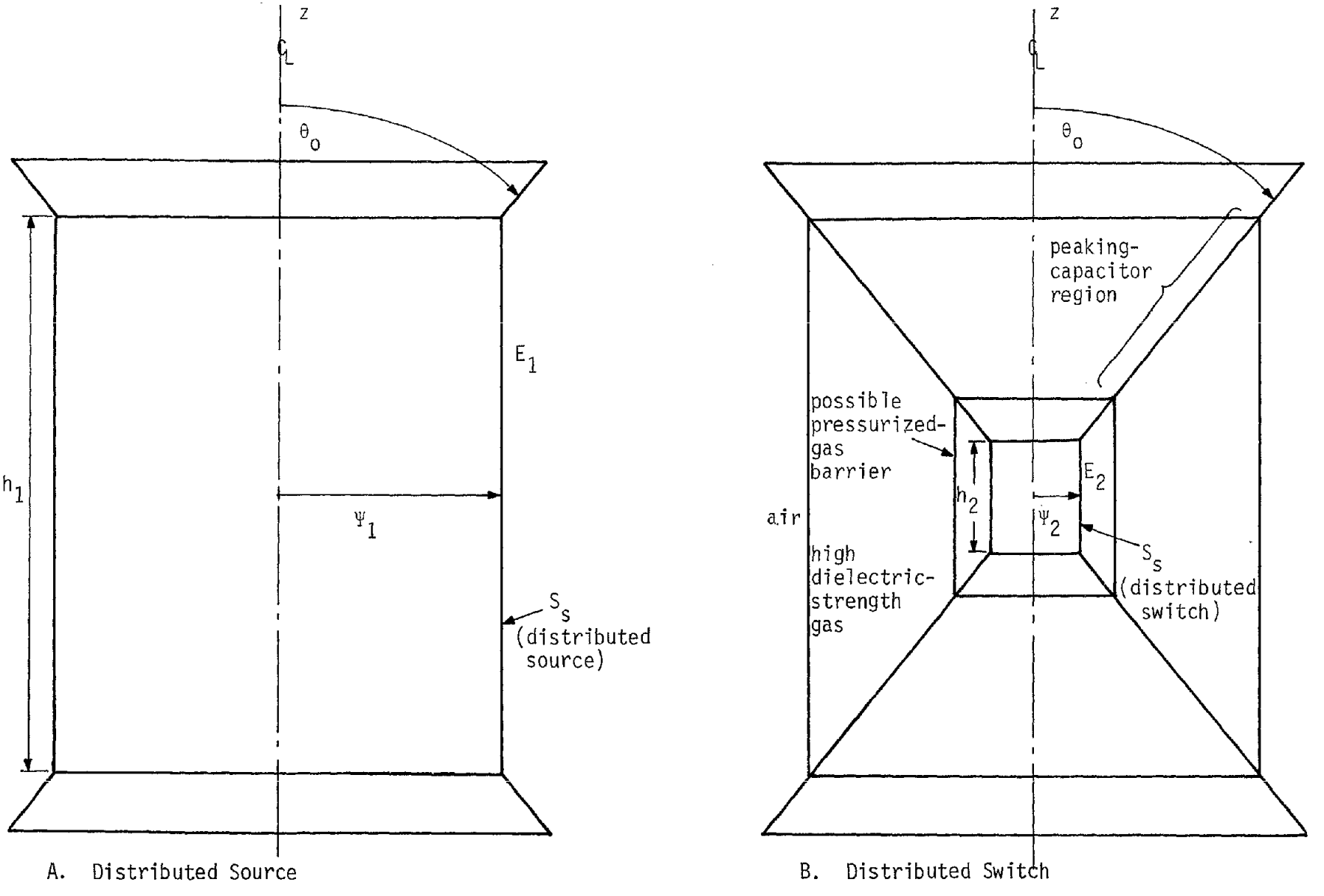

Figure 4.1. Comparison of Distributed Source and Distributed Switch.

$$N_2 = \frac{h_2}{\Delta_2} \frac{2\pi\Psi_2}{\delta_2} \tag{4.2}$$

Comparing these two cases the distributed switch can have fewer switches than the distributed source by the ratio

$$\frac{N_2}{N_1} = \frac{h_2}{h_1} \frac{\Delta_1}{\Delta_2} \frac{\Psi_2}{\Psi_1} \frac{\delta_1}{\delta_2} \tag{4.3}$$

Now for simplicity let us assume that the requisite switch spacings for EM performance be the same, i.e.

$$\Delta_1 \equiv \Delta_2 \ , \ \delta_1 \equiv \delta_2 \tag{4.4}$$

giving

$$\frac{N_2}{N_1} = \frac{h_2}{h_1} \frac{\Psi_2}{\Psi_1} \tag{4.5}$$

Next let the cone angle θ_o be the same in both cases so that

$$\frac{h_2}{h_1} = \frac{\Psi_2}{\Psi_1} \tag{4.6}$$

giving

$$\frac{N_2}{N_1} = \left(\frac{h_2}{h_1}\right)^2 \tag{4.7}$$

This reduces the question to the relative size of h_2 and h_1. Roughly speaking, as one reduces radius from Ψ_1 to Ψ_2 the magnitude of the peak electric field increases proportionately from E_1 to E_2 as

$$\frac{h_2}{h_1} = \frac{E_1}{E_2} \tag{4.8}$$

This gives

$$\frac{N_2}{N_1} = \left(\frac{E_1}{E_2}\right)^2 \tag{4.9}$$

Suppose now that in reducing Ψ_1 to Ψ_2 with the attendant use of higher-dielectric-strength media (special gases, including pressurization) the peak electric field to be produced (or collapsed) by the distributed source (switch) is increased by say, one order magnitude. Then per (4.9) the requisite number of switches is decreased by a corresponding two orders of magnitude.

Consider now more features of the distributed switch as shown in fig. 4.2. The source surface S_s, while a body of revolution in this analysis, is not necessarily a cylinder (a point to be considered later). This source surface is divided into various smaller portions containing elementary switches and associated devices. As in fig. 4.2A conducting structures such as grading rings (and perhaps associated disks) can be incorporated in the switch structure as long as they do not short out the electric fields between one θ value on S_s and another such θ value. These conductors can be used to separate S_s into bands (see [1]) which are in effect bodies of revolution which contain some number of switches in parallel which are all triggered to close at the same time.

Fig. 4.2B shows a blowup of portions of these bands, schematically illustrating how a switch and grading resistors (plus various other equipment) forms a unit cell, $2\pi\Psi_2/\delta_2$ of which form one band. Note that separate bands are in general triggered at separate times to meet the requirements of the TEM wave in section 2.

The distributed switch differs from the earlier-considered distributed source in an interesting respect. The distributed source involves construction of a tangential electric field on S_s from a condition of a previously (approximately) null field on S_s. The

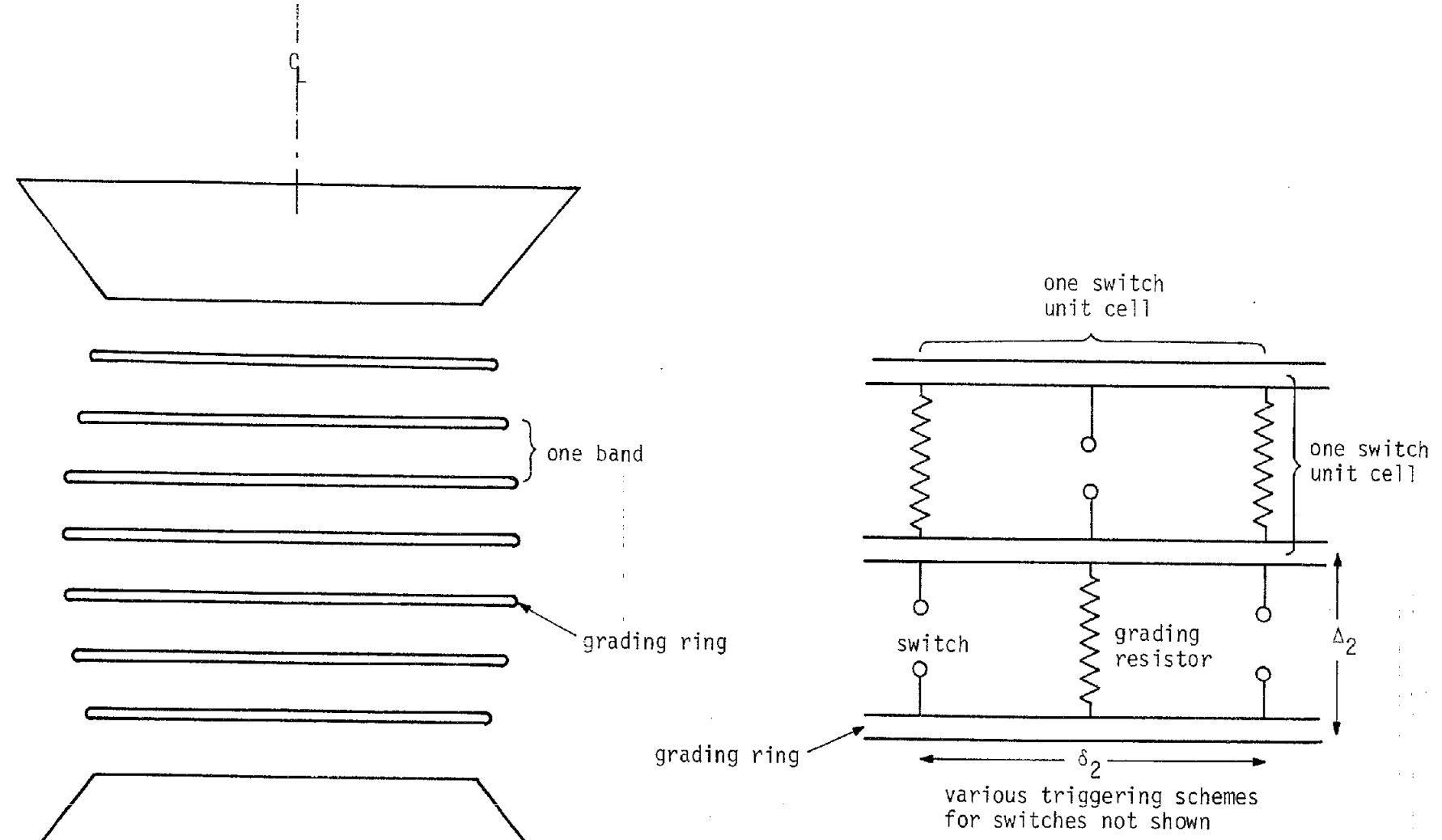

A. Distributed Source

B. Portion of Distributed Switch (Schematic, staggered switch arrangement)

Figure 4.2. Structure of Distributed Switch

distributed switch operates under a condition of a previously constructed quasi-static electric field in the switch region from the erection of the Marx generator into the peaking capacitors. Triggering the various switches in the distributed switch array brings about the collapse of the electric field in the switch region which has been established by the Marx generator in conjunction with elements such as the grading resistors. In effect S_s is transformed on triggering the switches into a highly conducting (shorted) sheet. The wave propagation into the interior of S_s is of a polarity to reduce the electric field there (with perhaps some overshoot). This feature might be useful in reducing high-voltage breakdown problems.

V. Cylindrical and Spherical Shapes for a Distributed Source/Switch

While the concept of a distributed source relies on closed boundary surfaces (including infinity) on which the tangential electric field is specified, there may be reasons why some particular shape of all or part of such a surface may be desirable for some purpose. In the context of high electric fields, electrical breakdown can be a problem, particulary near the source surface in the case of an expanding wave as in section 2. Furthermore, on (or near) S_s there is various equipment including switches, grading rings which perhaps are the "edges" of conducting disks (inside S_s) on which triggering equipment might be mounted, etc. One might then try to minimize the maximum electric fields on and near S_s in some sense.

A. Cylindrical

If as in [1] one sets the peak electric field magnitude to be uniform over S_s, then from (2.2) we have

$$\begin{aligned} |\vec{E}|_{\substack{\max \\ t}} &= |E_\theta|_{\substack{\max \\ t}} = \frac{|V_o|}{r} f_E(\theta) \\ &= |V_o| \left\{ r \sin(\theta) \, \ell n \left[\cot\left(\frac{\theta_o}{2}\right) \right] \right\}^{-1} \\ &= |V_o| \left\{ \Psi \, \ell n \left[\cot\left(\frac{\theta_o}{2}\right) \right] \right\}^{-1} \\ &\equiv E_o = \text{constant} \end{aligned} \tag{5.1}$$

which implies

$$\Psi \equiv \text{constant} \equiv \Psi_o \tag{5.2}$$

$S_s \equiv$ right circular cylinder of radius Ψ_o

Now on S_s the tangential electric field is just E_z which takes the form (at time of local peak)

$$|E_z| = -\frac{|V_o|}{r} f_o(\theta)\, \vec{I}_\theta \cdot \vec{I}_z$$

$$= |V_o| \left\{ \Psi_o \, \ell n \left[\cot\left(\frac{\theta_o}{2}\right) \right] \right\}^{-1} \sin(\theta)$$

$$= E_o \sin(\theta) = E_o \frac{\Psi_o}{r} = E_o \frac{\Psi_o}{\left[\Psi^2 + z^2\right]^{1/2}} \qquad (5.3)$$

Thus the maximum tangential electric field on S_s is just E_o, but away from $\theta = \pi/2$ the tangential electric field is less. As discussed in [1] if one takes equal voltage decrements on S_s for sources (or switches), then the widths of the associated bands (or the spacing between grading rings is nonuniform on S_s, increasing as one goes away from $\theta = \pi/2$.

B. Spherical

Another shape one might investigate for S_s is the sphere. In this case the magnitude of the electric field and of its tangential component just outside S_s is

$$|\vec{E}|_{\substack{\max \\ t}} = |E_\theta|_{\substack{\max \\ t}} = \frac{|V_o|}{\Psi_o} f_E(\theta) \qquad (5.4)$$

$$= \frac{|V_o|}{\Psi_o \sin(\theta)} \left\{ \ell n \left[\cot\left(\frac{\theta_o}{2}\right) \right] \right\}^{-1}$$

$\Psi_o \equiv$ radius of sphere S_s

Note how this field is proportional to $1/\sin(\theta)$ on S_s, increasing as one goes away from $\theta = \pi/2$ toward the circular conical conductors.

If one looks at the potential function (voltage) along S_s and requires equal voltage change between adjacent grading rings (as in fig. 4.2), then the grading rings space closer together as one approaches the circular conducting cones. This could be inconvenient for the design of switches, etc. Inside S_s there may be various equipment

(such as for triggering) required. If the grading rings are the outer "edges" of conducting disks then the disks near the circular conducting cones (away from $\theta < \pi/2$) will be considerably closer together and the electric fields (now z directed) inside S_s will be much higher in these extremities (near the conducting cones).

VI. Shape for Distributed Source/Switch with a Uniform Quasi-Static z-Directed Electric Field Inside S_s

One possible design consideration for a distributed source/switch is to maintain a uniform quasi-static electric field in the z direction inside S_s. Except for certain phenomena associated with fast transients, this could be important in designing the switches and triggering equipment associated with each band. If there are metallic circular disks whose "edges" are the grading rings, then these disks being perpendicular to the z axis, the electric field inside S_s is constrained to be approximately parallel to the z axis. Spacing these disks equally with equal voltages per band leads to this particular design.

Letting (in a peak sense between adjacent disks)

$$V = Az_c \quad , \quad A = \text{constant} \tag{6.1}$$

on S_s (and inside S_s in a quasi-static sense), we have from section 2 the corresponding voltage for our desired wave on S_s

$$V(\theta_c) = V_o \, f_V(\theta_c)$$

$$f_V(\theta) = \frac{\ell n\left[\cot\left(\frac{\theta}{2}\right)\right]}{\ell n\left[\cot\left(\frac{\theta_o}{2}\right)\right]} \tag{6.2}$$

where a subscript c denotes values on the contour in the (Ψ,z) plane corresponding to S_s.

Noting that

$$f_E(\theta) = -\frac{d}{d\theta} f_V(\theta)$$

$$= \left\{\sin(\theta)\, \ell n\left[\cot\left(\frac{\theta_o}{2}\right)\right]\right\}^{-1} \tag{6.3}$$

let us make S_s be perpendicular to the (x,y) plane (or $z = 0$ plane) at the intersection with this plane. At $z = 0$ then let us constrain that the electric field tangential to S_s be the same from both (6.1) and (6.2) giving

$$\begin{aligned}\frac{dV}{dz_c} &= A \\ &= -\frac{1}{\Psi_o}\left.\frac{dV}{d\theta_c}\right|_{\theta_c = \frac{\pi}{2}} \\ &= \frac{1}{\Psi_o} V_o f_E\left(\frac{\pi}{2}\right) \\ &= \frac{1}{\Psi_o} V_o \left\{\ell n\left[\cot\left(\frac{\theta_o}{2}\right)\right]\right\}^{-1}\end{aligned} \tag{6.4}$$

$\Psi_o \equiv$ radius of S_s on (x,y) plane

Equating the voltages in (6.1) and (6.2) on S_s we have

$$V_o \frac{\ell n\left[\cot\left(\frac{\theta_c}{2}\right)\right]}{\ell n\left[\cot\left(\frac{\theta_o}{2}\right)\right]} = \frac{z_c}{\Psi_o} V_o \left\{\ell n\left[\cot\left(\frac{\theta_o}{2}\right)\right]\right\}^{-1} \tag{6.5}$$

$$\frac{z_c}{\Psi_o} = \ell n\left[\cot\left(\frac{\theta_c}{2}\right)\right]$$

In spherical coordinates we have on S_s

$$\begin{aligned} z_c &= r_c \cos(\theta_c) \\ \frac{r_c}{\Psi_o} &= \frac{1}{\cos(\theta_c)} \ell n\left[\cot\left(\frac{\theta_c}{2}\right)\right]\end{aligned} \tag{6.6}$$

giving r_c/Ψ_o as a function of θ_c.

An alternate representation in cylindrical coordinates uses

$$\theta_c = 2\,\mathrm{arccot}\left(e^{\frac{z_c}{\Psi_o}}\right)$$

$$\frac{\Psi_c}{z_c} = \tan(\theta_c) \tag{6.7}$$

$$\frac{\Psi_c}{z_c} = \tan\left[2\,\mathrm{arccot}\left(e^{\frac{z_c}{\Psi_o}}\right)\right]$$

This is simplified by use of the trigonometric formula [12]

$$\tan(2a) = \frac{2}{\cot(a) - \tan(a)} \tag{6.8}$$

giving

$$\frac{\Psi_c}{z_c} = 2\left\{\cot\left[\mathrm{arccot}\left(e^{\frac{z_c}{\Psi_o}}\right)\right] - \tan\left[\mathrm{arccot}\left(e^{\frac{z_c}{\Psi_o}}\right)\right]\right\}^{-1}$$

$$= 2\left\{e^{\frac{z_c}{\Psi_o}} - e^{-\frac{z_c}{\Psi_o}}\right\}^{-1} \tag{6.9}$$

$$= \frac{1}{\sinh\left(\frac{z_c}{\Psi_o}\right)}$$

Thus we have

$$\frac{\Psi_c}{\Psi_o} = \frac{z_c}{\Psi_o}\left\{\sinh\left(\frac{z_c}{\Psi_o}\right)\right\}^{-1} \tag{6.10}$$

giving Ψ_c/z_o as an explicit function of z_c/Ψ_o.

Note that

$$\frac{\Psi_c}{\Psi_o} \leq 1$$

$$\left.\frac{\Psi_c}{\Psi_o}\right|_{z_c = 0} = 1 \tag{6.11}$$

Expanding (6.10) for small z_c/Ψ_o gives [12]

$$\frac{\Psi_c}{\Psi_o} = \frac{z_c}{\Psi_o}\left\{\frac{z_c}{\Psi_o} + \frac{1}{6}\left(\frac{z_c}{\Psi_o}\right)^3 + O\left(\left(\frac{z_c}{\Psi_o}\right)^5\right)\right\}^{-1}$$

$$= \left\{1 + \frac{1}{6}\left(\frac{z_c}{\Psi_o}\right)^2 + O\left(\left(\frac{z_c}{\Psi_o}\right)^4\right)\right\}^{-1}$$

$$= 1 - \frac{1}{6}\left(\frac{z_c}{\Psi_o}\right)^2 + O\left(\left(\frac{z_c}{\Psi_o}\right)^4\right) \qquad (6.12)$$

The constraint in this section produces a barrel shape for S_s. The maximum cylindrical radius is $\Psi = \Psi_o$ on the (x,y) plane with Ψ decreasing as z_c goes away from zero toward either of the circular conducting cones ($\Psi = \Psi_o$ and $\theta = \pi - \theta_o$).

VII. Shape for a Distributed Source/Switch with a Uniform Peak Tangential Electric Field on S_s

Another consideration might be that the spacing between the grading rings as in fig. 4.2A be uniform along S_s so that switches and grading resistors as in fig. 4.2B be all identical and tangential to S_s. With equal peak voltages between adjacent grading rings, or equivalently (to a good approximation) a uniform peak tangential component of $\vec{E}$ on S_s, one can determine a corresponding shape for S_s. Note of course that rotation symmetry (ϕ independence) of the field expressed in cylindrical coordinates implies that S_s is a body of revolution and that we need only specify a curve in the (Ψ,z) plane to specify S_s, as indicated in fig. 7.1.

Again the desired potential distribution on S_s (peak, neglecting retarded-time effects) is

$$V(\theta_c) = V_o\, f_V(\theta_c)$$

$$f_V(\theta) = \frac{\ell n\left[\cot\left(\frac{\theta}{2}\right)\right]}{\ell n\left[\cot\left(\frac{\theta_o}{2}\right)\right]} \qquad (7.1)$$

The corresponding electric field is

$$\vec{E} = -\frac{1}{r}\frac{dV}{d\theta}\vec{1}_\theta = \frac{V_o}{r} f_E(\theta)\,\vec{1}_\theta$$

$$f_E(\theta) = -\frac{d}{d\theta} f_V(\theta) \qquad (7.2)$$

$$= \left\{\sin(\theta)\ \ell n\left[\cot\left(\frac{\theta_o}{2}\right)\right]\right\}^{-1}$$

The unit tangent vector on S_s is

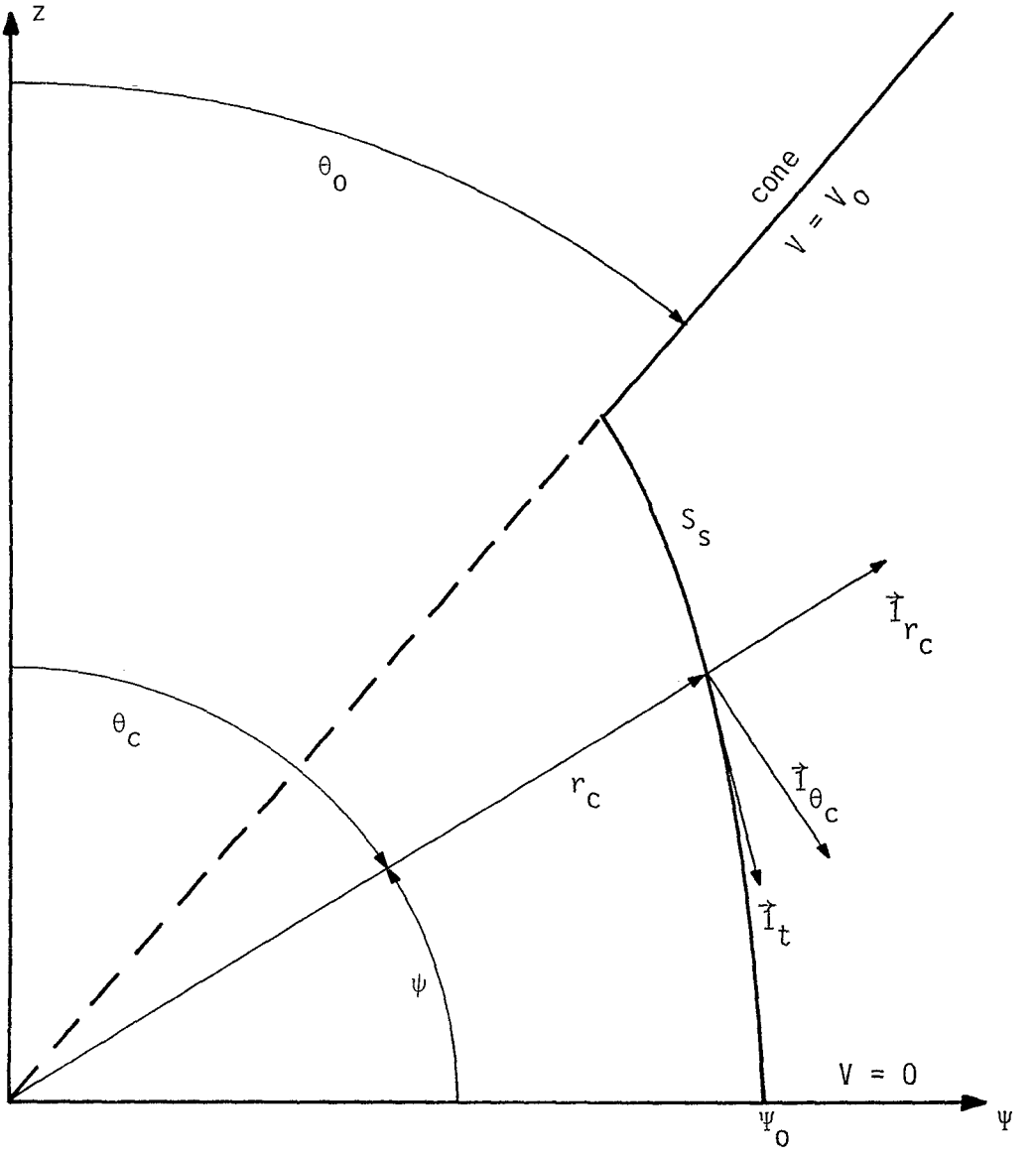

Figure 7.1. Coordinates for Distributed Source/Switch with Uniform Tangential Electric Field on S_s

$$\vec{I}_t = \left|\frac{d\vec{r}_c}{d\theta_c}\right|^{-1} \frac{d\vec{r}_c}{d\theta_c}$$

$$\frac{d\vec{r}_c}{d\theta_c} = \frac{d}{d\theta_c}\left[r_c \vec{I}_{r_c}\right] = \frac{dr_c}{d\theta_c}\vec{I}_{r_c} + r_c \frac{d}{d\theta_c}\vec{I}_{r_c} \qquad (7.3)$$

$$= \frac{dr_c}{d\theta_c}\vec{I}_{r_c} + r_c \vec{I}_{\theta_c}$$

The tangential electric field on S_s (peak) is then

$$E_t = \frac{V_o}{r_c} f_E(\theta_c)\, \vec{I}_{\theta_c} \cdot \vec{I}_t$$

$$= V_o\, f_E(\theta_c)\left\{\left(\frac{dr_c}{d\theta_c}\right)^2 + r_c^2\right\}^{-1/2} \qquad (7.4)$$

$$= E_o = \text{constant}$$

At $\theta_c = \pi/2$ set $r_c = \Psi_o$ and set $E_\theta = E_o$ (making the contour (and thus S_s) parallel to $\vec{E}$ here) giving

$$E_o = V_o \left\{\ell n\left[\cot\left(\frac{\theta_o}{2}\right)\right]\right\}^{-1}\left\{\left(\frac{dr_c}{d\theta_c}\right)^2\Bigg|_{r_c = \Psi_o} + \Psi_o^2\right\}^{-1/2} \qquad (7.5)$$

Using the symmetry of S_s with respect to the (x,y) plane so that

$$\left.\frac{dr_c}{d\theta_c}\right|_{\theta_c = \frac{\pi}{2}} = 0 \qquad (7.6)$$

gives

$$E_o = \frac{V_o}{\Psi_o}\left\{\ell n\left[\cot\left(\frac{\theta_o}{2}\right)\right]\right\}^{-1} \qquad (7.7)$$

Setting

$$R \equiv \frac{r_c}{\Psi_o} \tag{7.8}$$

then (7.4) becomes

$$f_E(\theta_c)\left\{\left(\frac{dR}{d\theta_c}\right)^2 + R^2\right\}^{-1/2} = \left\{\ell n\left[\cot\left(\frac{\theta_o}{2}\right)\right]\right\}^{-1}$$

$$\frac{1}{\sin(\theta_c)}\left\{\left(\frac{dR}{d\theta_c}\right)^2 + R^2\right\}^{-1/2} = 1 \tag{7.9}$$

or

$$1 = \sin(\theta_c)\left\{\left(\frac{dR}{d\theta_c}\right)^2 + R^2\right\}^{1/2} \tag{7.10}$$

with the initial conditions

$$\left.R\right|_{\theta_c = \frac{\pi}{2}} = 1$$

$$\left.\frac{dR}{d\theta_c}\right|_{\theta_c = \frac{\pi}{2}} = 0 \tag{7.11}$$

Defining

$$\psi \equiv \frac{\pi}{2} - \theta_c \tag{7.12}$$

then ψ represents the angle on S_s with respect to the symmetry plane $z = 0$. Then (7.10) becomes

$$1 = \cos(\psi)\left\{\left(\frac{dR}{d\psi}\right)^2 + R^2\right\}^{1/2} \tag{7.13}$$

or

$$\left(\frac{dR}{d\psi}\right)^2 + R^2 = \sec^2(\psi) \tag{7.14}$$

This first order nonlinear differential equation together with

$$\begin{aligned} R\Big|_{\psi = 0} &= 1 \\ \frac{dR}{d\psi}\Big|_{\psi = 0} &= 0 \end{aligned} \tag{7.15}$$

gives R as a function of ψ.

Now to better understand the functional form of $R(\psi)$ let us make series expansions as

$$\begin{aligned} R(\psi) &= \sum_{n=0}^{\infty,2} a_n \psi^n = a_o + a_2 \psi^2 + O(\psi^4) \\ \frac{dR(\psi)}{d\psi} &= \sum_{n=0}^{\infty,2} n\, a_n \psi^{n-1} = 2a_2\psi + O(\psi^3) \end{aligned} \tag{7.16}$$

Note that $R(\psi)$ has only even terms in the expansion due to the symmetry enforced with respect to $\psi = 0$ (or $z_c = 0$). Similarly in (7.14) we expand

$$\begin{aligned} \sec^2(\psi) &= \left\{1 + \frac{\psi^2}{2} + O(\psi^4)\right\}^2 \\ &= 1 + \psi^2 + O(\psi^4) \\ R^2(\psi) &= a_o^2 + 2a_o a_2 \psi^2 + O(\psi^4) \\ \left(\frac{dR(\psi)}{d\psi}\right)^2 &= 4\, a_2^2 \psi^2 + O(\psi^4) \end{aligned} \tag{7.17}$$

Substituting these expansions in (7.14) we have for the constant term

$$a_o^2 = 1$$
$$a_o = 1 \tag{7.18}$$

where the positive square root assures $R = 1$ at $\psi = 0$ as in (7.15). The ψ^2 term has

$$4 a_2^2 + 2 a_o a_2 = 1$$
$$4 a_2^2 + 2 a_2 - 1 = 0 \tag{7.19}$$
$$a_2 = \frac{-2 \pm \sqrt{4 + 16}}{8} = \frac{-1 \pm \sqrt{5}}{4}$$

Choosing the positive square root so that R increases with ψ^2 gives

$$a_2 = \frac{-1 + \sqrt{5}}{4} \simeq .309$$
$$R = 1 + \frac{-1 + \sqrt{5}}{4} \psi^2 + O(\psi^4) \tag{7.20}$$

In cylindrical coordinates we have

$$R = \left\{\left(\frac{\Psi_c}{\Psi_o}\right)^2 + \left(\frac{z_c}{\Psi_o}\right)^2\right\}^{1/2} = \frac{\Psi_c}{\Psi_o}\left\{1 + \frac{1}{2}\left(\frac{z_c}{\Psi_c}\right)^2 + O\left(\left(\frac{z_c}{\Psi_c}\right)^4\right)\right\}$$
$$\psi^2 = \left\{\arctan\left(\frac{z_c}{\Psi_c}\right)\right\}^2 = \left\{\frac{z_c}{\Psi_c} + O\left(\left(\frac{z_c}{\Psi_c}\right)^3\right)\right\}^2 \tag{7.21}$$
$$= \left(\frac{z_c}{\Psi_c}\right)^2 + O\left(\left(\frac{z_c}{\Psi_c}\right)^4\right)$$

Then (7.20) becomes

$$\frac{\Psi_c}{\Psi_o}\left\{1+\frac{1}{2}\left(\frac{z_c}{\Psi_c}\right)^2+0\left(\left(\frac{z_c}{\Psi_c}\right)^4\right)\right\}=1+\frac{-1+\sqrt{5}}{4}\left\{\left(\frac{z_c}{\Psi_c}\right)^2+0\left(\left(\frac{z_c}{\Psi_c}\right)^4\right)\right\}$$

$$\frac{\Psi_c}{\Psi_o}=\left\{1+\frac{-1+\sqrt{5}}{4}\left(\frac{z_c}{\Psi_c}\right)^2+0\left(\left(\frac{z_c}{\Psi_c}\right)^4\right)\right\}\left\{1-\frac{1}{2}\left(\frac{z_c}{\Psi_c}\right)^2+0\left(\left(\frac{z_c}{\Psi_c}\right)^4\right)\right\}$$

$$=1+\frac{-3+\sqrt{5}}{4}\left(\frac{z_c}{\Psi_c}\right)^2+0\left(\left(\frac{z_c}{\Psi_c}\right)^4\right) \qquad (7.22)$$

On the right side substituting for Ψ_c gives

$$\frac{\Psi_c}{\Psi_o}=1+\frac{-3+\sqrt{5}}{4}\left(\frac{z_c}{\Psi_o}\right)^2+0\left(\left(\frac{z_c}{\Psi_o}\right)^4\right)$$

$$\frac{-3+\sqrt{5}}{4}\cong -0.191 \qquad (7.23)$$

$$\frac{\Psi_c}{\Psi_o}\simeq 1-0.191\left(\frac{z_c}{\Psi_o}\right)^2 \quad \text{for small} \quad \frac{z_c}{\Psi_o}$$

A numerical solution of (7.14) with the conditions of (7.15) is easily effected by rewriting (7.14) as

$$\frac{dR}{d\psi}=-\left[\sec^2(\psi)-R^2\right]^{1/2} \qquad (7.24)$$

beginning at $\psi = 0$, $R = 1$ and incrementing through increasing ψ as $\psi + \Delta\psi$ with the next R as $R + (dR/d\psi)\Delta\psi$. If $\Delta\psi$ is taken sufficiently small the function $R(\psi)$ converges to the desired accuracy, as can be determined by varying $\Delta\psi$ and noting an insignificant change in $R(\psi)$.

The function $R(\psi)$ is tabulated in tables 7.1 and 7.2 for the bicone impedance $Z_c = 120\Omega$ and $Z_c = 150\Omega$ respectively. Here the corresponding cone angles are determined through the formulae of section 2 together with

$$Z_c = Z_o f_g$$

$$f_g = \frac{1}{\pi} \ell n\left[\cot\left(\frac{\theta_o}{2}\right)\right]$$

$$Z_o = \sqrt{\frac{\mu_o}{\varepsilon_o}}$$

$$\mu_o \equiv 4\pi \times 10^{-7} \text{ H/m}$$

$$\varepsilon_o = \frac{1}{\mu_o c^2}$$

$$c = 2.99793\ (\pm 10^{-5}) \times 10^8 \text{ m/s} \quad \text{(measured speed of light)}$$

Then we have

$$\begin{aligned} Z_c = 120\Omega &\Rightarrow \theta_o \simeq 0.7045 \text{ radians} \\ &\simeq 40.37 \text{ degrees} \\ Z_c = 150\Omega &\Rightarrow \theta_o \simeq 0.5576 \text{ radians} \\ &\theta_o \simeq 31.95 \text{ degrees} \end{aligned} \qquad (7.26)$$

In these tables the independent variable is taken as f_V for $\theta_o \leq \theta \leq \pi/2$ or $0 \leq \psi \leq \pi/2 - \theta_o$. Uniform decrements of f_V are taken since one may typically use uniform voltages for the distributed source/switch under consideration.

Figure 7.2 summarizes the shape of this and other choices for S_s, plotting Ψ_c/Ψ_o versus z_c/z_o for cylindrical and spherical shapes (section 5) as well as the shapes discussed in section 6 and the present section.

f_V	$\psi = \frac{\pi}{2} - \theta$ radians	θ radians	R	$\frac{\Psi}{\Psi_o}$	$\frac{Z}{\Psi_o}$
Ø.ØØ	Ø.ØØØ	1.57Ø7	1.ØØØØØ	1.ØØØØØØ	Ø.ØØØØ
Ø.Ø1	Ø.Ø1Ø	1.56Ø7	1.ØØØ1Ø	1.ØØØØ5Ø	Ø.Ø1ØØ
Ø.Ø2	Ø.Ø2Ø	1.55Ø7	1.ØØØ24	1.ØØØØ41	Ø.Ø2ØØ
Ø.Ø3	Ø.Ø3Ø	1.54Ø7	1.ØØØ44	Ø.999995	Ø.Ø3ØØ
Ø.Ø4	Ø.Ø4Ø	1.53Ø7	1.ØØØ71	Ø.999911	Ø.Ø4ØØ
Ø.Ø5	Ø.Ø5Ø	1.52Ø7	1.ØØ1Ø4	Ø.999789	Ø.Ø5ØØ
Ø.Ø6	Ø.Ø6Ø	1.51Ø7	1.ØØ143	Ø.999629	Ø.Ø6ØØ
Ø.Ø7	Ø.Ø69	1.5ØØ8	1.ØØ188	Ø.999430	Ø.Ø7ØØ
Ø.Ø8	Ø.Ø79	1.49Ø8	1.ØØ239	Ø.999193	Ø.Ø8ØØ
Ø.Ø9	Ø.Ø89	1.48Ø8	1.ØØ297	Ø.998919	Ø.Ø9ØØ
Ø.1Ø	Ø.Ø99	1.47Ø8	1.ØØ361	Ø.998606	Ø.1ØØØ
Ø.11	Ø.1Ø9	1.46Ø9	1.ØØ43Ø	Ø.998255	Ø.11Ø1
Ø.12	Ø.119	1.451Ø	1.ØØ5Ø6	Ø.997866	Ø.12Ø1
Ø.13	Ø.129	1.441Ø	1.ØØ589	Ø.997439	Ø.13Ø1
Ø.14	Ø.139	1.4311	1.ØØ677	Ø.996975	Ø.14Ø1
Ø.15	Ø.149	1.4212	1.ØØ772	Ø.996473	Ø.15Ø1
Ø.16	Ø.159	1.4113	1.ØØ872	Ø.995933	Ø.16Ø1
Ø.17	Ø.169	1.4Ø14	1.ØØ979	Ø.995356	Ø.17Ø1
Ø.18	Ø.179	1.3916	1.Ø1Ø92	Ø.994741	Ø.18Ø1
Ø.19	Ø.188	1.3818	1.Ø1211	Ø.994089	Ø.19Ø1
Ø.2Ø	Ø.198	1.3719	1.Ø1336	Ø.993400	Ø.2ØØ1
Ø.21	Ø.2Ø8	1.3621	1.Ø1467	Ø.992674	Ø.21Ø1
Ø.22	Ø.218	1.3524	1.Ø16Ø4	Ø.991911	Ø.22Ø1
Ø.23	Ø.228	1.3426	1.Ø1747	Ø.991112	Ø.23Ø1
Ø.24	Ø.237	1.3329	1.Ø1897	Ø.99Ø276	Ø.24Ø1
Ø.25	Ø.247	1.3231	1.Ø2Ø52	Ø.989403	Ø.25Ø1
Ø.26	Ø.257	1.3135	1.Ø2214	Ø.988495	Ø.26ØØ
Ø.27	Ø.266	1.3Ø38	1.Ø2381	Ø.987550	Ø.27ØØ
Ø.28	Ø.276	1.2941	1.Ø2555	Ø.986569	Ø.28ØØ
Ø.29	Ø.286	1.2845	1.Ø2734	Ø.985553	Ø.29ØØ
Ø.3Ø	Ø.295	1.2749	1.Ø2920	Ø.984502	Ø.3ØØØ
Ø.31	Ø.3Ø5	1.2654	1.Ø3111	Ø.983415	Ø.3Ø99
Ø.32	Ø.314	1.2559	1.Ø3308	Ø.982293	Ø.3199
Ø.33	Ø.324	1.2464	1.Ø3512	Ø.981136	Ø.3299
Ø.34	Ø.333	1.2369	1.Ø3721	Ø.979945	Ø.3398
Ø.35	Ø.343	1.2275	1.Ø3936	Ø.978719	Ø.3498
Ø.36	Ø.352	1.218Ø	1.Ø4157	Ø.977459	Ø.3597
Ø.37	Ø.362	1.2Ø87	1.Ø4384	Ø.976165	Ø.3697
Ø.38	Ø.371	1.1993	1.Ø4617	Ø.974838	Ø.3796
Ø.39	Ø.38Ø	1.19ØØ	1.Ø4855	Ø.973477	Ø.3896
Ø.4Ø	Ø.389	1.18Ø7	1.Ø5100	Ø.972Ø83	Ø.3995
Ø.41	Ø.399	1.1715	1.Ø5350	Ø.97Ø656	Ø.4Ø95
Ø.42	Ø.4Ø8	1.1623	1.Ø56Ø6	Ø.969196	Ø.4194
Ø.43	Ø.417	1.1531	1.Ø5868	Ø.967704	Ø.4293
Ø.44	Ø.426	1.144Ø	1.Ø6135	Ø.966180	Ø.4392
Ø.45	Ø.435	1.1349	1.Ø64Ø7	Ø.964625	Ø.4492
Ø.46	Ø.444	1.1259	1.Ø6688	Ø.963Ø37	Ø.4591
Ø.47	Ø.453	1.1169	1.Ø6972	Ø.961419	Ø.469Ø
Ø.48	Ø.462	1.1Ø79	1.Ø7263	Ø.959769	Ø.4789

Table 7.1 Distibuted Source/Switch with Uniform Tangential Electric Field on S_s : Z_c = 120 Ω.

f_V	$\psi = \frac{\pi}{2} - \theta$ radians	θ radians	R	$\frac{\Psi}{\Psi_o}$	$\frac{z}{\Psi_o}$
Ø.49	Ø.471	1.Ø99Ø	1.Ø7559	Ø.958Ø89	Ø.4888
Ø.5Ø	Ø.48Ø	1.Ø9Ø1	1.Ø786Ø	Ø.956378	Ø.4987
Ø.51	Ø.489	1.Ø812	1.Ø8168	Ø.954637	Ø.5Ø86
Ø.52	Ø.498	1.Ø724	1.Ø8481	Ø.952867	Ø.5185
Ø.53	Ø.5Ø7	1.Ø636	1.Ø8799	Ø.951Ø67	Ø.5283
Ø.54	Ø.515	1.Ø549	1.Ø9123	Ø.949238	Ø.5382
Ø.55	Ø.524	1.Ø462	1.Ø9452	Ø.947380	Ø.5481
Ø.56	Ø.533	1.Ø376	1.Ø9787	Ø.945494	Ø.558Ø
Ø.57	Ø.541	1.Ø29Ø	1.1Ø128	Ø.943579	Ø.5678
Ø.58	Ø.55Ø	1.Ø7Ø4	1.1Ø474	Ø.941637	Ø.5777
Ø.59	Ø.558	1.Ø119	1.1Ø825	Ø.939667	Ø.5875
Ø.6Ø	Ø.567	1.ØØ35	1.11182	Ø.937670	Ø.5974
Ø.61	Ø.575	Ø.995Ø	1.11544	Ø.935646	Ø.6Ø72
Ø.62	Ø.584	Ø.9867	1.11911	Ø.933595	Ø.6171
Ø.63	Ø.592	Ø.9783	1.12284	Ø.931518	Ø.6269
Ø.64	Ø.6ØØ	Ø.97Ø1	1.12662	Ø.929416	Ø.6367
Ø.65	Ø.6Ø8	Ø.9618	1.13Ø46	Ø.927287	Ø.6465
Ø.66	Ø.617	Ø.9537	1.13434	Ø.925134	Ø.6564
Ø.67	Ø.625	Ø.9455	1.13828	Ø.922955	Ø.6662
Ø.68	Ø.633	Ø.9374	1.14227	Ø.92Ø753	Ø.676Ø
Ø.69	Ø.641	Ø.9294	1.14632	Ø.918525	Ø.6858
Ø.7Ø	Ø.649	Ø.9214	1.15Ø41	Ø.916275	Ø.6956
Ø.71	Ø.657	Ø.9134	1.15456	Ø.914ØØØ	Ø.7Ø54
Ø.72	Ø.665	Ø.9Ø55	1.15875	Ø.911Ø3	Ø.7152
Ø.73	Ø.673	Ø.8977	1.163ØØ	Ø.9Ø9382	Ø.7249
Ø.74	Ø.68Ø	Ø.8899	1.16730	Ø.9Ø7Ø39	Ø.7347
Ø.75	Ø.688	Ø.8821	1.17165	Ø.9Ø4674	Ø.7445
Ø.76	Ø.696	Ø.8744	1.176Ø5	Ø.9Ø2287	Ø.7543
Ø.77	Ø.7Ø3	Ø.8668	1.18Ø49	Ø.899879	Ø.764Ø
Ø.78	Ø.711	Ø.8592	1.18499	Ø.897450	Ø.7738
Ø.79	Ø.719	Ø.8516	1.18954	Ø.895ØØØ	Ø.7835
Ø.8Ø	Ø.726	Ø.8441	1.19413	Ø.892530	Ø.7933
Ø.81	Ø.734	Ø.8367	1.19878	Ø.89ØØ39	Ø.8Ø3Ø
Ø.82	Ø.741	Ø.8293	1.2Ø347	Ø.887529	Ø.8128
Ø.83	Ø.748	Ø.8219	1.2Ø821	Ø.884999	Ø.8225
Ø.84	Ø.756	Ø.8146	1.213ØØ	Ø.882451	Ø.8322
Ø.85	Ø.763	Ø.8Ø74	1.21784	Ø.879884	Ø.8419
Ø.86	Ø.77Ø	Ø.8ØØ1	1.22272	Ø.877298	Ø.8517
Ø.87	Ø.777	Ø.793Ø	1.22765	Ø.874695	Ø.8614
Ø.88	Ø.784	Ø.7859	1.23263	Ø.872Ø74	Ø.8711
Ø.89	Ø.791	Ø.7788	1.23765	Ø.869435	Ø.88Ø8
Ø.9Ø	Ø.798	Ø.7718	1.24272	Ø.866780	Ø.89Ø5
Ø.91	Ø.8Ø5	Ø.7649	1.24783	Ø.864Ø8	Ø.9ØØ2
Ø.92	Ø.812	Ø.758Ø	1.253ØØ	Ø.861419	Ø.9Ø99
Ø.93	Ø.819	Ø.7511	1.2582Ø	Ø.858715	Ø.9196
Ø.94	Ø.826	Ø.7443	1.26345	Ø.855995	Ø.9292
Ø.95	Ø.833	Ø.7376	1.26875	Ø.853260	Ø.9389
Ø.96	Ø.839	Ø.73Ø9	1.27Ø9	Ø.85Ø51Ø	Ø.9486
Ø.97	Ø.846	Ø.7242	1.27947	Ø.847746	Ø.9583
Ø.98	Ø.853	Ø.7176	1.28490	Ø.844967	Ø.9679
Ø.99	Ø.859	Ø.711Ø	1.29Ø37	Ø.842174	Ø.9776
1.ØØ	Ø.866	Ø.7Ø45	1.29589	Ø.839367	Ø.9873

Table 7.1 Continued and Concluded.

f_V	$\psi = \frac{\pi}{2} - \theta$ radians	θ radians	R	$\frac{\Psi}{\Psi_o}$	$\frac{z}{\Psi_o}$
0.00	Ø.ØØØ	1.57Ø7	1.ØØØØØ	1.ØØØØØØ	Ø.ØØØØ
Ø.Ø1	Ø.Ø12	1.5582	1.ØØØ15	1.ØØØØ78	Ø.Ø125
Ø.Ø2	Ø.Ø25	1.5457	1.ØØØ37	1.ØØØØ64	Ø.Ø25Ø
Ø.Ø3	Ø.Ø37	1.5332	1.ØØØ69	Ø.999993	Ø.Ø375
Ø.Ø4	Ø.Ø5Ø	1.52Ø7	1.ØØ111	Ø.999861	Ø.Ø5ØØ
Ø.Ø5	Ø.Ø62	1.5Ø82	1.ØØ162	Ø.999671	Ø.Ø625
Ø.Ø6	Ø.Ø74	1.4958	1.ØØ223	Ø.999420	Ø.Ø75Ø
Ø.Ø7	Ø.Ø87	1.4833	1.ØØ294	Ø.999110	Ø.Ø875
Ø.Ø8	Ø.Ø99	1.47Ø8	1.ØØ374	Ø.998740	Ø.1ØØ1
Ø.Ø9	Ø.112	1.4584	1.ØØ464	Ø.998311	Ø.1126
Ø.1Ø	Ø.124	1.446Ø	1.ØØ563	Ø.997822	Ø.1251
Ø.11	Ø.137	1.4336	1.ØØ673	Ø.997275	Ø.1376
Ø.12	Ø.149	1.4212	1.ØØ791	Ø.996668	Ø.15Ø1
Ø.13	Ø.161	1.4Ø88	1.ØØ92Ø	Ø.996ØØ2	Ø.1626
Ø.14	Ø.174	1.3965	1.Ø1Ø57	Ø.995278	Ø.1751
Ø.15	Ø.186	1.3842	1.Ø12Ø5	Ø.994496	Ø.1876
Ø.16	Ø.198	1.3719	1.Ø1362	Ø.993655	Ø.2ØØ1
Ø.17	Ø.211	1.3597	1.Ø1528	Ø.992756	Ø.2127
Ø.18	Ø.223	1.3475	1.Ø17Ø4	Ø.991800	Ø.2252
Ø.19	Ø.235	1.3353	1.Ø189Ø	Ø.99Ø787	Ø.2376
Ø.2Ø	Ø.247	1.3231	1.Ø2Ø84	Ø.989716	Ø.25Ø1
Ø.21	Ø.259	1.311Ø	1.Ø2289	Ø.988589	Ø.2626
Ø.22	Ø.271	1.299Ø	1.Ø25Ø2	Ø.987405	Ø.2751
Ø.23	Ø.283	1.2869	1.Ø2726	Ø.986165	Ø.2876
Ø.24	Ø.295	1.2749	1.Ø2958	Ø.984870	Ø.3ØØ1
Ø.25	Ø.3Ø7	1.263Ø	1.Ø32ØØ	Ø.983519	Ø.3125
Ø.26	Ø.319	1.2511	1.Ø3451	Ø.982114	Ø.325Ø
Ø.27	Ø.331	1.2393	1.Ø3711	Ø.98Ø654	Ø.3375
Ø.28	Ø.343	1.2275	1.Ø3981	Ø.979140	Ø.3499
Ø.29	Ø.355	1.2157	1.Ø4259	Ø.977572	Ø.3624
Ø.3Ø	Ø.366	1.2Ø4Ø	1.Ø4547	Ø.975952	Ø.3748
Ø.31	Ø.378	1.1923	1.Ø4845	Ø.974279	Ø.3873
Ø.32	Ø.389	1.18Ø7	1.Ø5151	Ø.972554	Ø.3997
Ø.33	Ø.4Ø1	1.1692	1.Ø5466	Ø.97Ø777	Ø.4121
Ø.34	Ø.413	1.1577	1.Ø579Ø	Ø.968949	Ø.4246
Ø.35	Ø.424	1.1463	1.Ø6124	Ø.967Ø71	Ø.437Ø
Ø.36	Ø.435	1.1349	1.Ø6466	Ø.965142	Ø.4494
Ø.37	Ø.447	1.1236	1.Ø6817	Ø.963164	Ø.4618
Ø.38	Ø.458	1.1124	1.Ø7177	Ø.961138	Ø.4742
Ø.39	Ø.469	1.1Ø12	1.Ø7546	Ø.959Ø62	Ø.4866
Ø.4Ø	Ø.48Ø	1.Ø9Ø1	1.Ø7924	Ø.956939	Ø.499Ø
Ø.41	Ø.491	1.Ø79Ø	1.Ø831Ø	Ø.954769	Ø.5114
Ø.42	Ø.5Ø2	1.Ø68Ø	1.Ø87Ø5	Ø.952552	Ø.5237
Ø.43	Ø.513	1.Ø571	1.Ø91Ø9	Ø.95Ø29Ø	Ø.5361
Ø.44	Ø.524	1.Ø462	1.Ø9522	Ø.947982	Ø.5484
Ø.45	Ø.535	1.Ø354	1.Ø9943	Ø.945629	Ø.56Ø8
Ø.46	Ø.546	1.Ø247	1.1Ø373	Ø.943232	Ø.5731
Ø.47	Ø.556	1.Ø14Ø	1.1Ø811	Ø.94Ø791	Ø.5855
Ø.48	Ø.567	1.ØØ35	1.11257	Ø.938Ø8	Ø.5978

Table 7.2 Distributed Source/Switch with Uniform Tangential Electric Field on S_s : Z_c = 150 Ω.

f_V	$\psi = \frac{\pi}{2} - \theta$ radians	θ radians	R	$\frac{\Psi}{\Psi_o}$	$\frac{z}{\Psi_o}$
Ø.49	Ø.577	Ø.9929	1.11712	Ø.935782	Ø.61Ø1
Ø.5Ø	Ø.588	Ø.9825	1.12176	Ø.933215	Ø.6224
Ø.51	Ø.598	Ø.9721	1.12648	Ø.93Ø6Ø6	Ø.6347
Ø.52	Ø.6Ø8	Ø.9618	1.13127	Ø.927958	Ø.647Ø
Ø.53	Ø.619	Ø.9516	1.13616	Ø.925270	Ø.6593
Ø.54	Ø.629	Ø.9415	1.14112	Ø.922543	Ø.6716
Ø.55	Ø.639	Ø.9314	1.14616	Ø.919777	Ø.6838
Ø.56	Ø.649	Ø.9214	1.15129	Ø.916975	Ø.6961
Ø.57	Ø.659	Ø.9115	1.15650	Ø.914135	Ø.7Ø84
Ø.58	Ø.669	Ø.9Ø16	1.16178	Ø.911258	Ø.72Ø6
Ø.59	Ø.678	Ø.8918	1.16714	Ø.9Ø8347	Ø.7329
Ø.6Ø	Ø.688	Ø.8821	1.17259	Ø.9Ø54ØØ	Ø.7451
Ø.61	Ø.698	Ø.8725	1.17811	Ø.9Ø2419	Ø.7573
Ø.62	Ø.7Ø7	Ø.863Ø	1.18371	Ø.899405	Ø.7695
Ø.63	Ø.717	Ø.8535	1.18938	Ø.896357	Ø.7817
Ø.64	Ø.726	Ø.8441	1.19513	Ø.893278	Ø.7939
Ø.65	Ø.735	Ø.8348	1.2ØØ96	Ø.89Ø166	Ø.8Ø61
Ø.66	Ø.745	Ø.8256	1.2Ø687	Ø.887Ø25	Ø.8183
Ø.67	Ø.754	Ø.8164	1.21284	Ø.883852	Ø.83Ø5
Ø.68	Ø.763	Ø.8Ø74	1.218Ø	Ø.88Ø651	Ø.8427
Ø.69	Ø.772	Ø.7984	1.225Ø2	Ø.877420	Ø.8548
Ø.7Ø	Ø.781	Ø.7894	1.23122	Ø.874162	Ø.867Ø
Ø.71	Ø.79Ø	Ø.78Ø6	1.23750	Ø.87Ø875	Ø.8791
Ø.72	Ø.798	Ø.7718	1.24384	Ø.867563	Ø.8913
Ø.73	Ø.8Ø7	Ø.7631	1.25Ø26	Ø.864223	Ø.9Ø34
Ø.74	Ø.816	Ø.7545	1.25675	Ø.86Ø859	Ø.9156
Ø.75	Ø.824	Ø.746Ø	1.263Ø	Ø.857469	Ø.9277
Ø.76	Ø.833	Ø.7376	1.26993	Ø.854Ø56	Ø.9398
Ø.77	Ø.841	Ø.7292	1.27663	Ø.85Ø619	Ø.9519
Ø.78	Ø.849	Ø.72Ø9	1.28339	Ø.847159	Ø.964Ø
Ø.79	Ø.858	Ø.7127	1.29Ø23	Ø.843676	Ø.9761
Ø.8Ø	Ø.866	Ø.7Ø45	1.29713	Ø.84Ø172	Ø.9882
Ø.81	Ø.874	Ø.6965	1.3Ø41Ø	Ø.836648	1.ØØØ3
Ø.82	Ø.882	Ø.6885	1.31114	Ø.833Ø3	1.Ø124
Ø.83	Ø.89Ø	Ø.68Ø6	1.31824	Ø.829538	1.Ø245
Ø.84	Ø.898	Ø.6727	1.32541	Ø.825954	1.Ø365
Ø.85	Ø.9Ø5	Ø.665Ø	1.33264	Ø.822351	1.Ø486
Ø.86	Ø.913	Ø.6573	1.33994	Ø.818731	1.Ø6Ø7
Ø.87	Ø.921	Ø.6497	1.34730	Ø.815Ø94	1.Ø727
Ø.88	Ø.928	Ø.6422	1.35472	Ø.811440	1.Ø848
Ø.89	Ø.936	Ø.6347	1.36221	Ø.8Ø777Ø	1.Ø968
Ø.9Ø	Ø.943	Ø.6273	1.36976	Ø.8Ø4Ø84	1.1Ø89
Ø.91	Ø.95Ø	Ø.62ØØ	1.37737	Ø.8ØØ384	1.12Ø9
Ø.92	Ø.957	Ø.6128	1.38504	Ø.796669	1.1329
Ø.93	Ø.965	Ø.6Ø56	1.39277	Ø.792941	1.145Ø
Ø.94	Ø.972	Ø.5985	1.4ØØ56	Ø.789200	1.157Ø
Ø.95	Ø.979	Ø.5915	1.4Ø842	Ø.785446	1.169Ø
Ø.96	Ø.986	Ø.5846	1.41633	Ø.781680	1.1810
Ø.97	Ø.993	Ø.5777	1.4243Ø	Ø.777902	1.1931
Ø.98	Ø.999	Ø.5709	1.43232	Ø.774114	1.2051
Ø.99	1.ØØ6	Ø.5642	1.44041	Ø.77Ø315	1.2171
1.ØØ	1.Ø13	Ø.5576	1.44855	Ø.766507	1.2291

Table 7.2 Continued and Concluded.

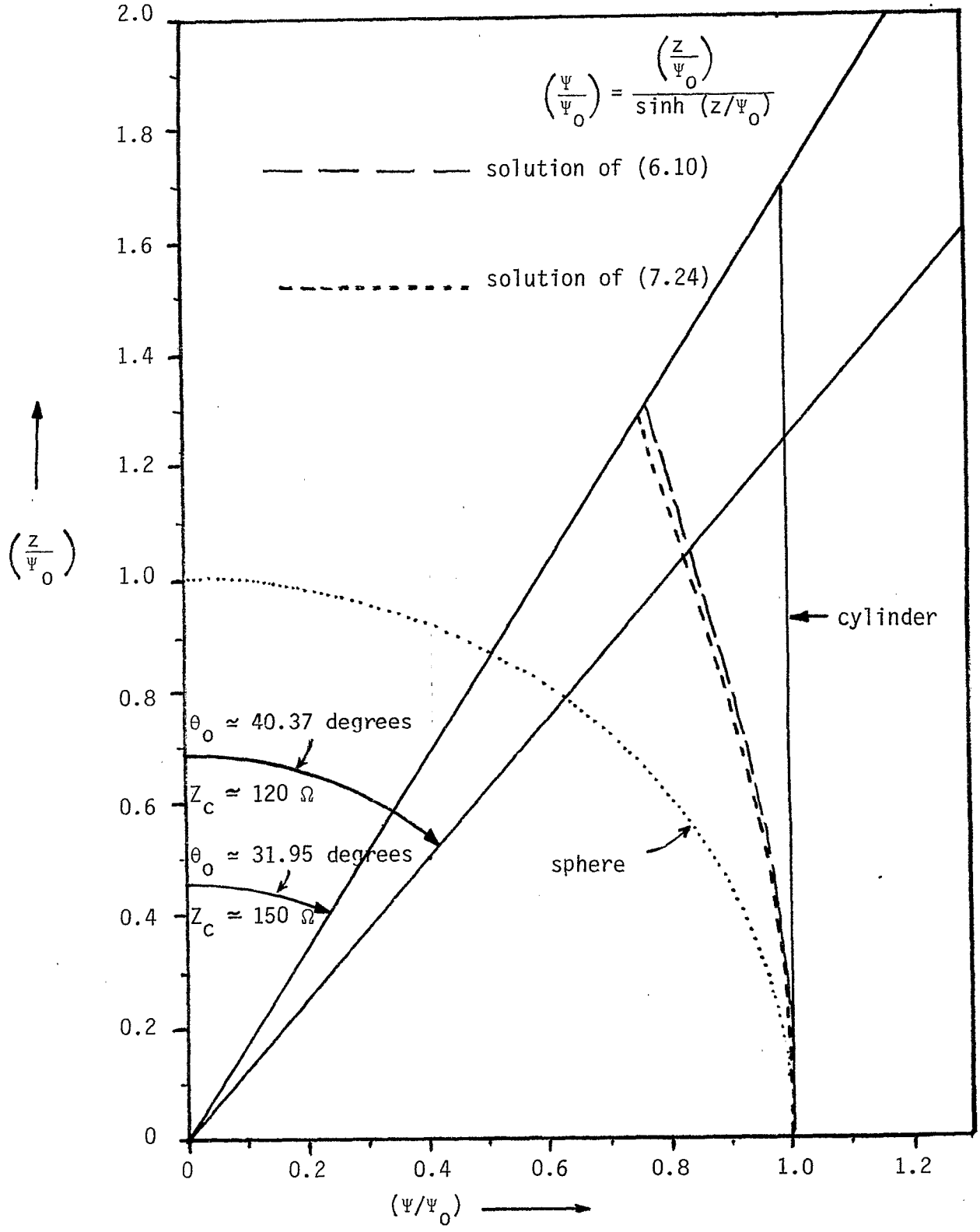

Figure 7.2 Various Shapes for Distributed Source/Switch

VIII. Summary

This paper has first extended the concept of a distributed source to that of a distributed switch. This has the potential benefit of greatly reducing the required number of switches by reducing the required size of the distributed source. In this scheme one may still use distributed peaking capacitors as is typically done in biconic pulser geometries. While this paper has addressed itself to the case of pulsers intended to drive biconic (or monoconic) antennas (at least near the pulser), the concept is not limited to this case and other types of distributed switches can be envisioned for other types of EMP simulator geometries.

In realizing a distributed source or switch for use in a biconic (or monoconic) geometry there are a variety of shapes which one can use to realize this. Here we have considered several shapes based on uniformity of various electric-field components near S_s. Depending on the relative practical importance of various design problems a particular shape can be selected.

References

1. C.E. Baum, The Distributed Source for Launching Spherical Waves, Sensor and Simulation Note 84, May 1969.

2. P.R. Barnes, Pulse Radiation by an Infinitely Long, Perfectly Conducting, Cylindrical Antenna in Free Space Excited by a Finite Cylindrical Distributed Source Specified by the Tangential Electric Field Associated with a Biconical Antenna, Sensor and Simulation Note 110, July 1970.

3. C.E. Baum, General Principles for the Design of ATLAS I and II, Part IV: Additional Considerations for the Design of Pulser Arrays, Sensor and Simulation Note 146, March 1972.

4. C.E. Baum, General Principles for the Design of ATLAS I and II, Part V: Some Approximate Figures of Merit for Comparing the Waveforms Launched by Imperfect Pulser Arrays onto TEM Transmission Lines, Sensor and Simulation Note 148, May 1972.

5. Z.L. Pyne and F.M. Tesche, Pulse Radiation by an Infinite Cylindrical Antenna with a Source Gap with a Uniform Field, Sensor and Simulation Note 159, October 1972.

6. F.M. Tesche and Z.L. Pyne, Approximation to a Biconical Source Feed on Linear EMP Simulators by Using N Discrete Voltage Gaps, Sensor and Simulation Note 175, May 1973.

7. C.E. Baum, Early Time Performance at Large Distances of Periodic Planar Arrays of Planar Bicones with Sources Triggered in a Plane-Wave Sequence, Sensor and Simulation Note 184, August 1973.

8. T.K. Liu, Admittances and Fields of a Planar Array with Sources Excited in a Plane Wave Sequence, Sensor and Simulation Note 186, October 1973.

9. C.E. Baum, EMP Simulators for Various Types of Nuclear EMP Environments: An Interim Categorization, Sensor and Simulation Note 240, January 1978, IEEE Trans. Antennas and Propagation, January 1978, pp. 35-53, and IEEE Trans. EMC, February 1978, pp. 35-53.

10. I.D. Smith and H. Aslin, Pulsed Power for EMP Simulators, IEEE Trans. Antennas and Propagation, January 1978, pp. 53-59, and IEEE Trans. EMC, February 1978, pp. 53-59.

11. J.A. Stratton, Electromagnetic Theory, McGraw Hill, 1941.

12. M. Abramowitz and I.A. Stegun, Handbook of Mathematical Functions, U.S. Gov't. Printing Office, 1964.